THE ASTROPHYSICAL JOURNAL, 401:49–59, 1992 December 10

A DISTANCE-INDEPENDENT CALIBRATION OF THE LUMINOSITY OF TYPE Ia SUPERNOVAE AND THE HUBBLE CONSTANT

BRUNO LEIBUNDGUT AND PHILIP A. PINTO[1]
Harvard-Smithsonian Center for Astrophysics, 60 Garden Street, Cambridge, MA 02138
Received 1992 January 31; accepted 1992 June 11

ABSTRACT

We present a calibration of the absolute magnitude of Type Ia supernovae (SNe Ia) at maximum by means of radioactive decay models for the light curve. Comparison of the calculated late time thermalized radiation with a bolometric light curve constructed from observations circumvents problems of modeling the complex physics that govern the peak phase and avoids the conversion of theoretical luminosities into filter magnitudes. The parameter space for the absolute magnitude is explored with several explosion models and a range of rise times. The absolute B magnitudes at maximum are then used to derive a range for the Hubble constant and the distance to the Virgo Cluster of galaxies from SNe Ia. Critical examination of the Hubble diagram of SNe Ia at peak yields rigorous limits for H_0 of 45 and 105 km s^{-1} Mpc^{-1}. Surprisingly, our determination of the value of H_0 is limited strongly by the unknown extinction toward individual supernovae. Improvements on the values of the Hubble constant from SNe Ia remain mainly in spectral modeling to find appropriate explosion models and in the use of near-infrared filters which are affected less by extinction.

Subject headings: distance scale — stars: abundances — stars: fundamental parameters — supernovae: general

1. INTRODUCTION

Not all Type Ia supernovae (SNe Ia) are identical in appearance (Phillips et al. 1987; Frogel et al. 1987; Branch, Drucker, & Jeffery 1988; Phillips et al. 1992); still, they are very similar, and this has prompted investigations into the use of SNe Ia as "standard candles" (Tammann 1982; Branch 1982; Cadonau, Sandage, & Tammann 1985; Branch 1985; Leibundgut & Tammann 1990, hereafter LT; Leibundgut 1991). Because they can be observed out to a redshift of about 0.5, they form promising candidates for measuring the cosmological deceleration parameter q_0 (e.g., Leibundgut 1990). Although their photometric uniformity (Leibundgut et al. 1991a) and the small scatter of their absolute magnitude at maximum seem to be well established (Kowal 1968; Tammann 1978; LT; Tammann & Leibundgut 1990, hereafter TL; Miller & Branch 1990; see, however, van den Bergh & Pazder 1992), an absolute calibration of the luminosity of SNe Ia is still lacking. Most determinations of this quantity rely on independent measurements of the distances to parent galaxies of SNe Ia and thus suffer from all the ambiguities involved with the use of a "cosmic distance ladder" in determining the extragalactic distance scale (cf. van den Bergh & Pritchett 1988). This problem was dramatically illustrated by the two discrepant determinations of $M_B^{\max}$, and hence H_0, by TL and by Fukugita & Hogan (1991) based upon the *same* sample of SNe. A new route for a distance-independent calibration of SNe Ia was pioneered by Arnett, Branch, & Wheeler (1985; hereafter ABW) and Branch (1992) who determined the absolute magnitudes of SNe Ia on the basis of explosion models.

Any method of distance measurement, but especially a "standard candle," must have a firm theoretical underpinning to be truly satisfactory. By standard candle we mean an easily recognizable class of phenomena whose intrinsic variation in luminosity is small compared with our ability to determine its uncertainty. The peak luminosity of SNe Ia seems to fit this definition quite well. Many attempts have been made to explain the apparent homogeneity of the SN Ia class. There is now general agreement (cf. Wheeler & Harkness 1990; Harkness & Wheeler 1990) that the thermonuclear model (see Woosley & Weaver 1986 for a review) provides such an explanation. In this view, a SN Ia is the thermonuclear explosion of a Chandrasekhar-mass carbon-oxygen (C/O) white dwarf (see, however, Shigeyama et al. 1992, who use a 1 $M_\odot$ white dwarf in their explosion scenario). Such models (Weaver, Axelrod, & Woosley 1980, hereafter WAW; Arnett 1982; Nomoto, Thielemann, & Yokoi 1984; Woosley & Weaver 1986) have been very successful in reproducing observed spectra both at maximum light (e.g., Harkness 1991a; Jeffery et al. 1992) and at late times (e.g., WAW; Pinto 1988); recent light curve calculations have been able to reproduce the observations as well (Harkness 1991b; Khokhlov, Müller, & Höflich 1992). There remain, however, important unresolved questions concerning the stellar evolution that lead to white dwarfs with such high masses (e.g., Iben & Tutukov 1984), and no candidate object has been found to date despite extensive searches (Bragaglia et al. 1990; Bragaglia, Greggio, & Renzini 1991).

The luminosity in the thermonuclear model is provided entirely by energy liberated in the decay of the radioactive isotope ^{56}Ni and its daughter product ^{56}Co produced by burning stellar material to nuclear statistical equilibrium (NSE). In any such model, the peak luminosity of a SN Ia is determined mainly by the amount of ^{56}Ni produced in the explosion. The importance of this connection between nucleosynthesis and observed luminosity was pointed out by ABW, who employed an analytic approximation for the peak luminosity (Arnett 1982) to derive a value for the Hubble constant using SNe Ia in elliptical galaxies. Several problems afflicting this approach center on the complexity of the light curve formation process during the photospheric phase of the supernova and the separation of the predicted luminosity into filter magnitudes. Simple assumptions, such as equating the instantaneous emission of the decay energy at maximum to the luminosity at peak and using truncated blackbodies to represent

[1] *Gamma Ray Observatory* Fellow.

the complex emergent spectrum, respectively, have been adopted in the past. Recently, Branch (1992) has surveyed the literature for the more successful models of SNe Ia, used their values of the peak luminosity, and employed an observed spectrum to derive an absolute B magnitude at maximum and a Hubble constant by this method.

We present a modification of the procedure outlined by ABW and Branch (1992) by employing theoretical calculations of γ-ray escape from the supernova's nebular phase and a bolometric light curve constructed from observations of several SNe Ia. The thermalized energy emanating from the explosion at late times (usually, if inaccurately, termed "bolometric luminosity") is the difference between the total energy produced by radioactive decay and the γ-ray luminosity. Such a light curve of thermalized radiation can be compared to the observed bolometric light curve at late epochs. Calculations of the light curve of SN 1987A based upon this γ-ray escape model have been quite successful (Woosley, Pinto, & Ensman 1988; Pinto & Woosley 1988; Woosley, Pinto, & Hartmann 1989; Suntzeff et al. 1992), and we expect that the model is even more accurate for the case of SNe Ia where sources of additional energy such as a central pulsar are not expected. After calculating a model's late time light curve, we find the absolute B magnitude of SNe Ia at maximum by extrapolating back along the *observed* bolometric light curve. This approach has the advantage that only relatively simple physical processes need be modeled and that the filter magnitudes are defined by the construction of the bolometric light curve.

With an absolute calibration of SNe Ia we are able to determine the distance to the Virgo Cluster of galaxies from the mean apparent peak magnitudes of SNe Ia in that cluster and the Hubble constant from the Hubble diagram of distant SNe Ia. Several uncertainties (e.g., peculiar velocities of the parent galaxies or extinction of individual SNe) set limits on the accuracy to which the Hubble parameter may be ascertained. With the luminosity known independently from distance measurements and a large enough sample of observations, SNe Ia may eventually be used to determine the infall velocity of the Local Group toward the Virgo Cluster of galaxies.

In this work we constrain the possible range of absolute peak luminosities we can derive for SNe Ia from models. For the comparison with observations, a bolometric light curve constructed from multifilter data (§ 2) is applied. The explosion models and their light curves are discussed in § 3. In § 4 the range of absolute luminosities and magnitudes is presented. The implications for the value of the Hubble constant as well as for the distance to the Virgo Cluster are discussed in § 5. The conclusions are presented in § 6.

2. THE OBSERVED BOLOMETRIC LIGHT CURVE

We have used template light curves in the six filters *UBVJHK* derived by Leibundgut (1988; see also Leibundgut & Tammann 1992, hereafter LT92) to construct a bolometric light curve for SNe Ia. These templates, which span the epochs from 5 days before until 110 days past the B maximum, were originally assembled in order to check the photometric homogeneity of SNe Ia, but they are also ideally suited for our purposes. Integration of the templates over wavelength provides a bolometric light curve covering the spectrum from $\sim$3500 Å to $\sim$2.2 μm. The agreement of the individual filter templates with observed photometry is exceedingly good in all filters for well-observed SNe (e.g., Leibundgut 1991; LT92; Hamuy et al. 1991; Wells et al. 1993; Leibundgut et al. 1991b) and supports the concept of SNe Ia as standard candles (for a comparison with all the available SNe I photometry see Leibundgut et al. 1991a). Small deviations ($\leq$0.2 mag) from the templates in B and V have been found by Phillips et al. (1992) for the well-observed SN 1991T. Recently, SN 1991bg displayed strong deviations from the templates in the B and V light curves (Leibundgut et al. 1993) in addition to severe differences in the $(B-V)$ color curve, the luminosity at maximum, and the spectral evolution at later times (Filippenko et al. 1992; Leibundgut et al. 1993).

Several problems are connected with the bolometric light curve constructed this way. First, we must use an intrinsic color for SNe Ia at a given epoch (typically the B maximum) to coordinate the templates. Primarily, the optical colors $(B-V)_0$ and $(U-B)_0$ are discussed in the literature (Pskovskii 1968; 1971; Barbon, Ciatti, & Rosino 1973; Cadonau et al. 1985; Capaccioli et al. 1990; LT92), and a wide range of values has been used. We applied $(B-V)_0 = -0.27$ mag and $(U-B)_0 = -0.40$ mag, based on the discussion in LT92. The infrared colors are measured for only a few SNe Ia (Elias et al. 1985; LT92). We used $(J-H)_0 = -1.36$ mag and $(H-K)_0 = 0.28$ mag as found by Leibundgut (1988). The infrared and optical regions are connected by $(B-H)_0$, which again relies on only a few SNe. Arguing that the bluest supernova [$(B-H)_0 = -0.87$ mag for SN 1972E] is likely to be least absorbed by dust, we chose to employ this value for the interpolation. The bolometric light curve, however, appears not to be very sensitive to the selection of these colors; it changes by only 8% for a choice of $(B-V)_0 = -0.15$ mag and $(U-B)_0 = -0.25$ mag. Changing $(B-H)_0$ by 0.1 mag also results in changes of less than 2% over the whole span of the templates.

Second, ultraviolet (shortward of 3200 Å) and the mid- and far-infrared emission (beyond 2.2 μm) are not included in our composite bolometric light curve. It is known that SNe Ia near maximum light are heavily line blanketed and have little UV emission compared with the optical (Blair & Panagia 1987). Panagia (1982) estimated the UV flux to be less than 10% of the overall emission at maximum. No SN Ia has ever been observed in the UV later than 2 weeks past maximum, but the temperatures measured from optical spectra appear so low that little emission at these wavelengths is expected at late times. The near-infrared emission (1.2–2.2 μm) is small compared with the total energies. It rises to nearly 10% around 30 days past B maximum, but is mostly less than 5%. Thus we expect only a small contribution from the infrared.

Third, there might be a concern that the interpolation between the V and J filter bands does not account for the emission in this region. Inspection of published R and I observations (Lee et al. 1972; Buta & Turner 1983) shows that the light curves in these bands are smooth interpolations between the V and J filters. The strong minimum in the J light curve (Elias et al. 1985) is weaker in I and only a plateau in the R light curves of SN 1972E and SN 1981B. The interpolation applied in the following, although increasing the uncertainties, should be an adequate representation of the data.

Finally, the use of broad-band filters for the integration tends to overestimate the bolometric luminosity for emission-line objects as described by Bouchet et al. (1991). This effect might play a role at late times for SNe Ia. It has been measured to amount to at most 10% for SN 1987A (Bouchet et al. 1991) and is probably of comparable size for SNe Ia.

The bolometric light curve from the integration of the light curve templates from Leibundgut (1988) is shown in Figure 1.

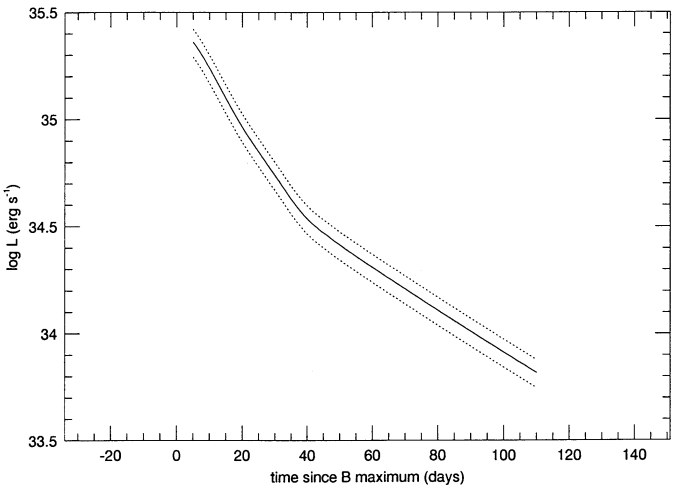

FIG. 1.—The bolometric light curve as constructed from individual filter light curves. The dotted lines delineate the adopted uncertainty (15%).

The luminosity is scaled to a B magnitude of 0.00 mag at B maximum. Unfortunately, no infrared observations are available around the maximum, and hence the peak of the bolometric light curve is not defined. Comparison with bolometric points for SN 1981B and SN 1972E (Graham 1987) shows excellent agreement between the shape of the light curve and observations (Leibundgut 1988). It is, however, hard to assess the contribution of the different uncertainties outlined above; an overall margin of $\pm 15\%$ (dotted lines in Fig. 1) should generously account for the cumulative effect of all of the uncertainties described above.

3. MODEL SUPERNOVAE AND LIGHT CURVES

The actual explosion energy in SNe Ia, that energy immediately released by explosive nuclear burning, can be inferred only indirectly. This is not the problem it seems at first; the essential fact behind using SNe Ia as distance indicators is that their *luminosity* is provided entirely by the subsequent decay of radioisotopes produced in the explosion. Rapid expansion from as compact a progenitor as a white dwarf ensures that all of the energy liberated by thermonuclear burning goes toward overcoming the gravitational binding energy of the star, accelerating the material of the ejecta. The single most important property for determining the luminosity of a SN Ia is thus the mass of radioisotopes it synthesizes. We know from spectroscopic evidence (Kirshner & Oke 1975; Axelrod 1980; WAW) and from the slope of the late time light curve (Clayton 1974; Colgate & McKee 1969) that a significant fraction ($\gtrsim 0.5$) of the material in the white dwarf is burnt to the iron group, with ^{56}Ni the most abundant radioactive product. This ^{56}Ni decays with a half-life of ~ 6 days to ^{56}Co, and the energy it releases is responsible for much of the luminosity at the peak of the light curve. ^{56}Co then decays to ^{56}Fe with a half-life of ~ 77 days, powering the light curve for at least the next few years.

The energetic radiation and particles emitted by radioactive decay either escape the ejecta altogether, or are absorbed and thermalized. In order to obtain an accurate estimate of the luminosity from a given supernova, we must adopt some model for the thermalization of the radioactive decay energy, its transport to the surface, and its eventual radiation into space. If the diffusion time of this thermalized energy is short compared with the elapsed time, it will eventually emerge as collisionally excited (thermal) emission in the near-ultraviolet, optical, and infrared. If the diffusion time is long compared with the elapsed time, however, the radiation is trapped in the rapidly expanding, optically thick ejecta and converted into kinetic energy of expansion (adiabatically degraded), and thus lost from the light curve. The luminosity at peak is determined by the competition between the escape of radiation from the supernova's surface and its adiabatic degradation. The time of maximum luminosity is thus determined by the diffusion time, which is in turn determined by the opacity of the ejecta. A larger opacity traps radiation for a longer time, giving the expansion more time to degrade the radiation into kinetic energy; the maximum in the light curve then occurs at a later time when the energy input from radioactive decay has decreased. ABW argued from Arnett's (1982) analytic models for SNe Ia light curves that the bolometric luminosity at maximum is *equal* to the radioactive decay luminosity at that instant. Using the range in nickel masses allowed by the thermonuclear model, they determined the range in the predicted maximum luminosity. This was an important step in placing the purely empirical use of SNe Ia as standard candles on a firmer theoretical foundation.

Numerical solution of the radiation hydrodynamic equations for the same explosion model but employing differing values of the optical opacity shows that the peak luminosity can change from that predicted by Arnett (1982) by substantial amounts (Branch 1992). Using the slightly more complex analytic model of WAW and Woosley, Taam, & Weaver (1986), we find that the ABW relation between time of maximum and instantaneous decay luminosity underestimates the peak luminosity for small values of the opacity (rapid rises to maximum) and overestimates this luminosity for large values (more gradual light curves). Khokhlov et al. (1992), using a much more detailed numerical treatment, find the same behavior. For the largest opacity employed by WAW, the analytic model overestimates the peak luminosity by 60%. Since even this value of the opacity produces too rapid a rise to peak (13 days as opposed to the observed 17–22 days discussed below), an even larger value of the opacity is indicated and the analytic prediction may be even further off the mark. In fact, it is the *time independence* of the assumed opacity which is in error. Improving upon these analytic models requires both a multifrequency time-dependent solution of the comoving frame transfer equation and a very large amount of atomic data for iron-group elements. Nonetheless, the trend is that more energetic explosions, with more rapid expansions and hence lower column depths at a given time, will peak earlier and at higher luminosities for a given ^{56}Ni mass.

A rather different technique was developed by Woosley et al. (1988), Pinto & Woosley (1988), and by Woosley, Pinto, & Hartmann (1989) to model the light curve of SN 1987A. While SN 1987A was a Type II supernova, all of its emission after approximately 30 days (Woosley 1988) derived from radioactive decay energy thermalized in its passage through the ejecta. Although simple, the model has continued to reproduce the light curve of SN 1987A up to the present time (Suntzeff et al. 1991, 1992). In this model, a detailed account is made of the escape and Comptonization of γ-rays produced by decay. Although it was initially developed to predict the X-ray and γ-ray light curve and spectrum, a by-product is the amount of energy that *does not* escape as high-energy radiation. Each Compton scattering yields a fast electron, and 19% of ^{56}Co decays yield a fast (≈ 600 keV) positron. The kinetic energy of

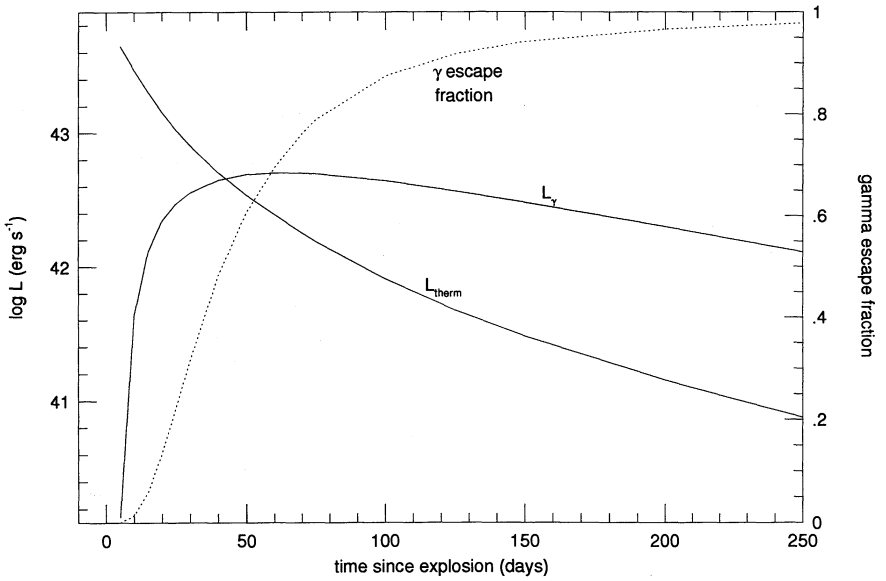

FIG. 2.—The luminosities of model DD3. The total luminosity is broken up into γ-ray luminosity and the thermalized radiation. The γ-escape fraction is indicated by the abscissa on the right side of the figure.

these particles is gradually shared among the material of the ejecta, mostly heating the ambient, thermal free electron gas. The gas is then cooled by emission of collisionally excited line radiation, leading to the observed "thermal" emission. The one assumption made in this model is that the time taken by the thermalization process is short compared with the time over which the luminosity changes and that little energy is lost to accelerating the expansion. For SNe Ia, these assumptions are abundantly satisfied following $\approx$60 days past explosion. After this date, the optical depth to thermalized radiation (as opposed to the Compton optical depth which can remain large), and hence the diffusion time, has decreased below one-tenth. The shape of the light curve is determined by the product of the exponentially decaying energy input and the increasing transparency, hence decreasing thermalization efficiency, of the ejecta (Fig. 2).

In Table 1 we present the explosion models considered in this paper. Column (2) gives the mass of unburned material that is left after the explosion, column (3) indicates the amount of intermediate-mass elements produced, while column (4) specifies the amount of ^{56}Ni synthesized in the explosion. The mass of iron-group isotopes is indicated in column (5). The kinetic energy available in a given model is displayed in column (6), while columns (7) and (8) describe the thermal luminosity at 60 and 100 days past explosion, respectively. The *e*-folding time for the luminosity between 60 and 100 days is indicated in column (9) for comparison with the value derived from the bolometric light curve. It is interesting to note that almost all models have declines that are slightly faster than the 43 days measured for the bolometric light curve. The "CDFA" models span a wide range of "classical" deflagrations, ignited on-center in Chandrasekhar-mass C/O white dwarfs (S. E. Woosley 1992, private communication). The "DD" models are typical of the so-called "delayed detonations" (Woosley 1991), and CDTG5 (Woosley et al. 1986) and W7 (Nomoto et al. 1984), both deflagrations, are typical of the current best attempts to fit all of the observations.

The rate at which the column depth declines is set by the expansion velocity of the ejecta. Because the nuclear burning that synthesizes the ^{56}Ni also overcomes the star's binding

TABLE 1

EXPLOSION MODELS FOR TYPE Ia SUPERNOVAE

Model[a] (1)	C + O $M_\odot$ (2)	Mg → Ca $M_\odot$ (3)	^{56}Ni $M_\odot$ (4)	"Fe" $M_\odot$ (5)	E_{kin} × 10^{51} ergs s (6)	$L(60)_{therm}$ × 10^{41} ergs s^{-1} (7)	$L(100)_{therm}$ × 10^{41} ergs s^{-1} (8)	τ_{60-100} days (9)
DD1	0.02	0.12	0.97	1.24	1.59	21.7	7.30	36.7
DD3	0.04	0.26	0.93	1.08	1.39	25.4	8.36	36.0
DD4	0.11	0.49	0.62	0.78	1.24	19.8	6.61	36.5
W7	0.18	0.27	0.63	0.87	1.19	19.4	6.54	36.8
CDTG5	0.46	0.10	0.51	0.88	1.05	15.4	5.06	35.9
CDFA4	0.99	0.03	0.20	0.37	0.12	16.2	8.86	66.3
CDFA5	0.52	0.09	0.52	0.78	0.86	17.7	5.77	35.7
CDFA6	0.02	0.01	0.98	1.08	1.66	22.3	7.33	36.0

NOTE.—All models were the result of exploding a Chandrasekhar-mass, C/O white dwarf. For each we give the masses of unburned C/O, partially burned material, ^{56}Ni, and the iron group, the kinetic energy of the explosion, the luminosity at 100 days past explosion (i.e., 80 $\pm$ 5 days past *B* maximum), and the slope of the 80–120 day light curve. Model CDTG5 was found to be the faintest computed to date and should provide a reasonable lower bound to the SN Ia luminosity at late times.

[a] The "DD" models are from Woosley (1991), W7 is taken from Nomoto, Thielemann, & Yokoi (1984), CDTG5 is from Woosley, Taam, & Weaver (1986), and the "CDFA" models are from Woosley (1992, private communication).

energy and determines this velocity, the two effects tend to work in opposition. For example, burning the entire star to NSE would lead to the production of nearly 1.4 $M_\odot$ of ^{56}Ni, but the consequent energetic explosion would lead to lower column depths, less γ-ray deposition, and hence a lower luminosity than such a large ^{56}Ni mass might otherwise have produced. Conversely, a much weaker explosion with a much smaller mass of ^{56}Ni would lead to a slower expansion, larger column depths, and hence a greater efficiency in converting decay energy to thermal radiation. ^{56}Ni is not the only result of burning in SNe Ia, however, and thus one cannot take this effect into account in a simple fashion. As an example of this behavior it is instructive to compare models DD3 and CDFA4 from Table 1. While DD3 produced nearly 5 times the ^{56}Ni of CDFA4 and 3 times as much iron-group material, the lower expansion velocity of CDFA4 leads to a much higher trapping efficiency, and the luminosity of these two models at 100 days past explosion differs by only 6%. Indeed, explosions such as CDTG5 which make $\sim 0.8\ M_\odot$ of iron-group elements yield the minimum luminosity for SNe Ia, about 5×10^{41} ergs s^{-1} at 100 days past explosion.

A rough limit for the fraction of the iron-group isotopes other than ^{56}Ni, which a successful model must produce, is provided by the abundances of iron isotopes in the solar system. If SNe Ia are to be responsible for the bulk of iron nucleosynthesis in Population I stars (Trimble 1982, 1991), the ratio of iron isotopes they produce must be near the solar value. This limits the fraction of the iron-group elements not produced as ^{56}Ni to less than $\sim 10\%$ for a typical SN Ia. Thus the kinetic energy and mass of radioactive ^{56}Ni are connected through the amount of material burned in the explosion. It is important to note that none of the models we consider satisfies the constraint set by iron-group isotopic nucleosynthesis. The effect of this is that the models have too little ^{56}Ni for their explosion energy and, hence, are systematically too faint.

A complicating factor is the production of intermediate-mass elements, the result of burning only partway to NSE. In many models, such as the deflagrations beginning with "CD" in Table 1, Mg, Si, S, Ar, and Ca are produced in quantities which are energetically unimportant. The so-called delayed detonation models ("DD") and deflagration model W7, however, produce such copious amounts of these elements (col. [3] in Table 1) that their kinetic energy is significantly increased. These models, with their greater γ-ray escape, are systematically fainter than the other deflagrations.

There are other constraints on the choice of models which depend only weakly on our knowledge of the specifics of the explosion. At the very least, the explosion must burn enough C/O to accelerate the outermost layers of the ejecta to the velocities observed in maximum light, and, more recently, pre-maximum spectra (Woosley & Weaver 1986; Leibundgut et al. 1991b; Jeffery et al. 1992). For central ignition of a weak deflagration in C/O dwarfs, this implies that $\gtrsim 0.35\ M_\odot$ of iron-group elements must be synthesized. On the other hand, lighter elements than the iron group are seen in early time spectra; indeed, the Si II λ6150 Å absorption is the defining property of the SN Ia class. Thus, the star cannot quite burn entirely to NSE. WAW also showed that detonations, in which nearly the entire mass of the white dwarf is burnt to ^{56}Ni, produced late time spectra that are far too highly ionized and exhibit far too broad line widths to represent real SNe Ia.

Because the faintest models possess an intermediate range of intrinsic properties, it is difficult to constrain the luminosity based on simple considerations. Nevertheless, the range of acceptable explosions can be limited by modeling the emergent spectra from SNe Ia. At early times, such models can constrain the abundance and velocity of intermediate mass elements (cf. Wheeler & Harkness 1990). At later times, synthetic spectra can be used to measure the overall kinetic energy of the explosion, the iron-group isotopic ratios, and the quantity of intermediate mass and unburned material present in the explosion. Such models are inherently quite complex, however, and are only now becoming calculable (Eastman & Pinto 1993). Several of the models in Table 1 can be ruled out upon consideration of their synthetic spectra. For example, the large mass of unburned oxygen in model CDFA4 leads to strong [O I]$\lambda\lambda$6300, 6363 Å doublet emission after 100 days, greatly exceeding the observational constraints. Model DD3, on the other hand, expands too rapidly and is too hot at late times, with higher average ionization of the iron group than observed. We have chosen for the present to ignore these results and examine the full range of models allowed by broader energetic constraints. A future paper will examine spectroscopic constraints in greater detail.

4. THE LUMINOSITY OF TYPE Ia SUPERNOVAE

With the data assembled in the previous sections we are now in a position to determine the range of luminosity and individual filter magnitudes from a comparison of the theoretical "thermal" and the observed bolometric light curves.

An important parameter for the evaluation of the luminosity at maximum is the time between explosion and the occurrence of maximum light in B (Δt). The value of Δt has not yet been determined by observations to an accuracy of better than a few days; we can get only lower limits from SNe observed at very early phases. The earliest observations of well-observed SNe Ia are reported for SN 1981D (Hamuy et al. 1991) and for SN 1990N (Leibundgut et al. 1991b). These are 15 and 17 days, respectively, before maximum in the B filter was attained. Other supernovae with early observations are SN 1961D, SN 1971G, and SN 1979B, all of which have been observed at least 18 days before maximum light (cf. Leibundgut et al. 1991a). The observations of these SNe, however, are plagued by uncertainties in the epoch of maximum. A loose upper limit for Δt of ~ 20 days was estimated by Leibundgut et al. (1991b).

Unfortunately, we can take no guidance from theoretical models of the early time light curve. Most models predict rise times of 7 to 10 days (Arnett 1982; Nomoto et al. 1984; WAW). Using an improved, time-dependent treatment of line blanketing, Harkness (1991b) has recalculated the rise time for model W7 to about 18 days. Only recently have models been created that take into account the longer rise times observed (Khokhlov et al. 1992; Shigeyama et al. 1991). These, however, invoke additional processes to prolong the rise and do not include complete time-dependent opacities.

Determining the absolute luminosity by matching the observed bolometric light curve with theoretical curves based upon γ-ray deposition does not provide a solution either. Thus, the rise time is a free parameter in our fits. Since these calculations are accurate only for epochs when the thermal diffusion time is short compared with the elapsed time, we compare the curves at epochs later than 40 days after maximum, when the bolometric light curve enters the final exponential decay. By extrapolating backward on the observed bolometric light curve, we can then determine the luminosities of SNe Ia at phases later than 5, but earlier than 40 days, past the B

TABLE 2

ABSOLUTE LUMINOSITIES FOR DIFFERENT EXPLOSION MODELS AND TIMES BETWEEN EXPLOSION AND MAXIMUM LIGHT

Model	Δt (days)	M_B^{max}	error	$L(5)^a$	error	$L(5)^b_{therm}$	$L(5)/L(5)_{therm}$
				$\times 10^{43}$ erg s^{-1}		$\times 10^{43}$ erg s^{-1}	
(1)	(2)	(3)	(4)	(5)	(6)	(7)	(8)
DD1	17	-19.492	0.043	1.43	0.058	1.25	0.87
	18	-19.456	0.039	1.40	0.051	1.16	0.83
	19	-19.438	0.036	1.36	0.046	1.09	0.80
	20	-19.412	0.032	1.33	0.040	1.02	0.77
	21	-19.385	0.029	1.30	0.035	0.96	0.74
	22	-19.359	0.027	1.27	0.032	0.91	0.72
DD3	17	-19.655	0.052	1.66	0.081	1.32	0.80
	18	-19.627	0.048	1.62	0.073	1.24	0.77
	19	-19.600	0.044	1.58	0.065	1.17	0.74
	20	-19.573	0.040	1.54	0.058	1.10	0.71
	21	-19.546	0.037	1.50	0.052	1.04	0.69
	22	-19.519	0.033	1.47	0.045	0.98	0.67
DD4	17	-19.396	0.050	1.31	0.062	0.97	0.74
	18	-19.369	0.047	1.28	0.056	0.91	0.71
	19	-19.342	0.043	1.25	0.051	0.86	0.69
	20	-19.315	0.040	1.22	0.046	0.82	0.67
	21	-19.288	0.037	1.19	0.041	0.78	0.66
	22	-19.261	0.034	1.16	0.037	0.74	0.64
W7	17	-19.384	0.047	1.30	0.058	0.95	0.73
	18	-19.357	0.043	1.26	0.075	0.90	0.71
	19	-19.330	0.040	1.23	0.046	0.85	0.69
	20	-19.303	0.037	1.20	0.042	0.80	0.67
	21	-19.277	0.034	1.17	0.037	0.76	0.65
	22	-19.250	0.031	1.15	0.033	0.72	0.63
CDTG5	17	-19.106	0.060	1.00	0.057	0.80	0.80
	18	-19.078	0.056	0.98	0.052	0.76	0.78
	19	-19.050	0.052	0.95	0.047	0.71	0.75
	20	-19.022	0.048	0.93	0.042	0.68	0.73
	21	-18.995	0.045	0.91	0.039	0.64	0.70
	22	-18.968	0.041	0.88	0.034	0.61	0.69
CDFA4	17	-19.589	0.156	1.56	0.241	0.34	0.22
	18	-19.568	0.154	1.54	0.235	0.32	0.21
	19	-19.550	0.152	1.51	0.227	0.31	0.21
	20	-19.532	0.149	1.49	0.219	0.30	0.20
	21	-19.515	0.147	1.46	0.212	0.29	0.20
	22	-19.496	0.146	1.44	0.207	0.28	0.19
CDFA5	17	-19.255	0.060	1.15	0.065	0.84	0.73
	18	-19.227	0.056	1.12	0.059	0.80	0.71
	19	-19.199	0.052	1.09	0.053	0.75	0.69
	20	-19.172	0.048	1.07	0.048	0.71	0.66
	21	-19.144	0.045	1.04	0.044	0.68	0.65
	22	-19.117	0.041	1.01	0.039	0.65	0.64
CDFA6	17	-19.510	0.051	1.46	0.070	1.33	0.91
	18	-19.483	0.046	1.42	0.061	1.25	0.88
	19	-19.456	0.042	1.38	0.054	1.18	0.86
	20	-19.429	0.038	1.35	0.048	1.10	0.81
	21	-19.402	0.035	1.32	0.043	1.04	0.79
	22	-19.376	0.032	1.29	0.039	0.98	0.76

[a] Luminosity at 5 days past *B* maximum as extrapolated back on the bolometric light curve.
[b] Thermal luminosity at 5 days past *B* maximum predicted by the γ-ray calculations.

maximum. Least-squares fits were performed of the model light curves to the observations. Table 2 presents the results of the calculations for the most likely rise times, 17 to 22 days. Columns (3) and (4) display the absolute B magnitude at maximum and its formal error of the mean, respectively. The corresponding luminosity at 5 days past maximum as extrapolated from the bolometric light curve with its error (col. [5] and [6]) should be compared to the predicted thermal luminosity at 5 days (col. [7]) and at 100 days past maximum (col. [8] in Table 1).

It is striking how small the fitting errors are, i.e., how well the two light curves fit each other for all explosion models. The slopes of the two curves coincide quite well (see above). This by itself indicates the accuracy of the comparatively simple γ-ray escape model; the slope of the bolometric light curve at this time does not just reflect the lifetime of radioactive ^{56}Co, but is rather its modulation by the increasing transparency of the supernova envelope to γ-rays (see Fig. 2). This is further exemplified by the relatively large errors for the fits with CDFA4; in this explosion only little material is burned and the small kinetic energy keeps the column depths high even for these late phases. The fact that the bolometric light curve has a significantly steeper slope at earlier phases (until $\lesssim 40$ days past maximum) indicates that energy deposited at earlier times within the supernova is still diffusing out; this increases the luminosity above the instantaneous deposited energy from the decay.

The bolometric light curve provides a luminosity ratio, roughly the ratio between the luminosity at 5 and 80 days past maximum, which has to be matched by any successful model of the light curves. This ratio is ~ 18 for the given epochs and corresponds to a decline of 3.1 mag. Since we are not attempt ing a fit to the early light curve we are not able to perform this test, but by comparing the predicted luminosity from the bolometric light curve $L(5)$ and the thermalized luminosity of the decays $L(5)_{\rm therm}$ at 5 days past maximum we can estimate the excess energy diffusing out of the supernova shortly after maximum (col. [8] of Table 2). The excess energy deduced this way is in agreement with the estimate by Branch (1992) for the most successful calculations of the early light curve.

The construction of the bolometric light curve is such that we can derive the absolute B magnitudes of SNe Ia. Note that the magnitudes at maximum are *not* determined by detailed calculation of a model spectral distribution but rather by the construction of the bolometric light curve described above. Due to the normalization of the bolometric light curve it is not necessary to know the total luminosity at peak (which is not measurable since the bolometric light curve does not cover this epoch). The quoted errors are due only to the differences in the shape of the two curves and are negligible compared to the uncertainties introduced by the unknown rise time and the range covered by the different explosion models.

Figure 3 displays the absolute B magnitude $M_B^{\rm max}$ at maximum versus Δt. All models show the trend of decreasing luminosity for longer rise times. The effect, however, is surprisingly small, if one considers the changes in opacity that would account for such a delay in the peak of SNe Ia light curves. The luminosity differences among the models are much more significant and amount to $\gtrsim 60\%$ for the most extreme models (DD3 and CDTG5).

5. THE HUBBLE CONSTANT AND THE DISTANCE TO VIRGO

The distance-independent calibration of SNe Ia allows us to determine the Hubble constant and, *independently*, the distance

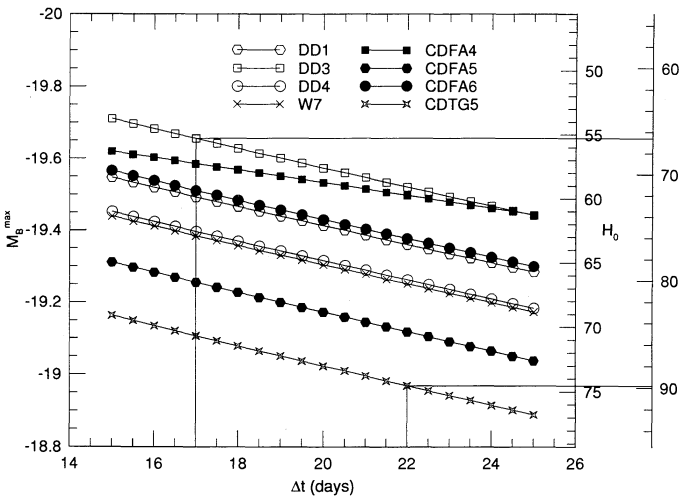

FIG. 3.—The dependence of the absolute luminosity on the different explosion models and the rise time (Δt). The scales on the right-hand side are solutions for the Hubble constant for different assumptions about extinction and intrinsic scatter of SNe Ia at maximum.

to the Virgo Cluster. The cosmic velocity of Virgo, when combined with current values of the infall velocity of the Local Group, then provides a test of the consistency between the data sets used for each determination. The advantage of this method, as pointed out by ABW and Branch (1992), is its complete independence from the "cosmic distance ladder." This allows us to circumvent the numerous problems which plague such approaches to distance measurement (cf. reviews in van den Bergh & Pritchett 1988).

With two independent samples of SNe Ia it is possible to decouple the determination of the Hubble constant and the Virgo distance, intimately related in recent discussions (Huchra 1988; Tammann 1988; Pierce & Tully 1988; Sandage & Tammann 1990). A sample of distant SNe (TL) provides the calibration for the Hubble constant and another of SNe in the Virgo Cluster gives a mean apparent B magnitude at maximum $m_B^{\rm max}$ (LT; Capaccioli et al. 1990).

The following discussion concentrates on the potential for using the luminosity of SNe Ia as direct indicators of distance. We will give an estimate of the range for the Hubble constant currently allowed by this method, and explore the uncertainties discussed above and inherent to the Hubble diagram of SNe Ia itself.

5.1. *The Hubble Constant from SNe Ia*

Determining the Hubble constant from the Hubble diagram of SNe Ia at maximum requires knowledge of the absolute peak magnitude of SNe Ia. Many authors have calibrated the absolute magnitudes of SNe Ia at peak scaled to the Hubble constant (Kowal 1968; Branch & Bettis 1978; van den Bergh 1988; Miller & Branch 1990). Using their determinations, scaled for the absolute magnitudes derived above, we find H_0 in the range from 53 to 63 km s^{-1} Mpc^{-1} ($M_B^{\rm max} = -19.7$) and 77 to 91 ($M_B^{\rm max} = -18.9$).

Tammann & Leibundgut (1990) have constructed a Hubble diagram with 34 SNe Ia observed in B. In order to avoid confusion with models of infall toward the Virgo Cluster, we have plotted in Figure 4 the same data using the heliocentric, rather than model-corrected, velocities. Adopting the same simple formulation of the problem as in TL, namely,

$$b = \log v - 0.2 m_B^{\rm max} , \qquad (1)$$

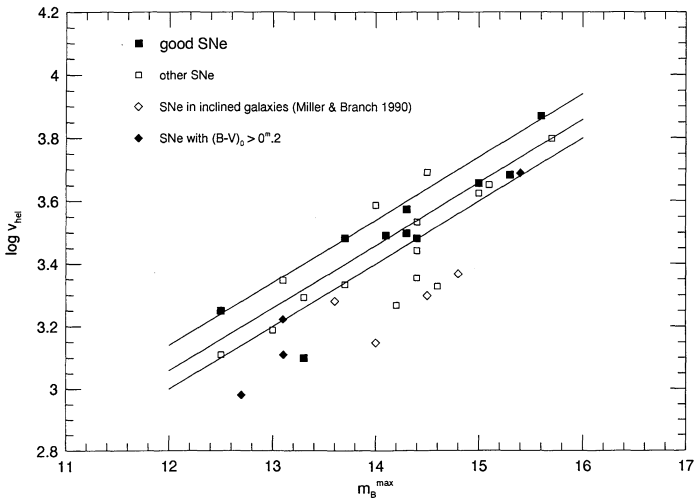

FIG. 4.—The Hubble diagram of SNe Ia at maximum. The sample is divided into supernovae with well-established B light curves ("good SNe"), SNe Ia with sufficient data to find a maximum ("other SNe"), and two groups of presumably heavily absorbed SNe Ia. The lines are solutions of the Hubble line of subsamples (see text).

we find from fitting the data from Figure 4 that $b = 0.600 \pm 0.021$ (error of the mean) for all 34 SNe (Table 3; lower line in Fig. 4). The fact that the error here is slightly higher than found by TL indicates that the infall model (Kraan-Korteweg 1986) successfully corrects for some velocity distortion caused by the gravitational potential of the Virgo Cluster.

Three sources of uncertainty prevent us from drawing firm conclusions from the observed distribution in the Hubble diagram: (1) the unknown contribution of peculiar velocities to the scatter around the Hubble line and hence b, (2) the as yet unknown intrinsic luminosity function of SNe Ia, and (3) the extinction of the SNe in the parent galaxy. An attempt to work out the first problem has been made by TL, and we will not repeat such an analysis here. The second problem cannot be treated right now and is also closely related to the third uncertainty which can be tackled at least approximately by using additional information on individual SNe. (1) and (2) can alter the derived value of b in either direction, while (3) only dims SNe and scatters the points (and the mean) toward fainter magnitudes.

All three effects can produce a selection bias in the sample. While the bias from the peculiar velocities is probably negligible, we must account for the incomplete sampling of the luminosity function, since there is a cutoff in apparent magnitude rather than a volume limit to the sample. In order to investigate the effect of bias introduced by extinction, we have identified in Figure 4 the four SNe that were found by Miller & Branch (1990) to lie in strongly inclined galaxies and which were underluminous in their sample. They clearly fall to the right of the line derived for the full set of SNe. In addition, SNe with $(B-V) > 0.2$ mag, presumably reddened by extinction, are specifically marked in Figure 4; again, these SNe fall mostly below the deduced Hubble line. To explore the influence of this bias we have calculated the parameter b for reduced sets of SNe, at the expense of increased statistical errors (Table 3). Somewhat surprisingly, the error in b is not decreased by excluding presumably absorbed supernovae from the sample, and even reaches a maximum for the set of SNe with the best determined light curves; this error is still well within the range of the systematic uncertainties, however. The middle line in Figure 4 is the mean from these 10 SNe (*filled squares*) and the large error results mainly from the one deviant point at $m_B = 13.3$ (SN 1967C).

The shifting of the lines toward brighter means could be interpreted as a Malmquist bias, i.e., the mean luminosity in the sample increases with distance. That such a selection bias is at work is also indicated by the decreased scatter around the Hubble line at large distances (TL), where obscured SNe have a smaller chance of being detected. It is not possible, with the relatively small number in the sample, to distinguish between a selection bias introduced by absorption and one caused by the intrinsic width of the luminosity distribution of SNe Ia. Such a distinction is very important for the derivation of the parameter b and thus the Hubble constant, because the two distributions result in very distinct biases. For a symmetric distribution such as a Gaussian variation in intrinsic luminosity, the "true" mean is measured as long as the objects are sampled completely in a given volume; the mean increases only when the sampling becomes incomplete. For such a distribution, it is therefore appropriate to fit to the mean of the sample. Averaging an asymmetric luminosity distribution, such as might result from extinction, can never retrieve the intrinsic luminosity of the distribution. To find the absolute "true" luminosity of such a distribution it is inappropriate to fit to the mean. Rather, we should have to compare the upper limit defined by the data with the absolute magnitude derived from the models.

There is thus no way to assess the "true" value of b without knowledge of the intrinsic luminosity function of SNe Ia at maximum and the influence of absorption on the observed distribution. The present data set cannot distinguish between

TABLE 3

THE HUBBLE PARAMETER b FOR VARIOUS SETS OF SNe Ia

SET (1)	b (2)	ERROR(b) (3)	N_{SNe} (4)	H_0 (km s^{-1} Mpc^{-1}) $-18.9 > M_B^{max} > -19.7$ (5)	(6)	v_{Virgo} (km s^{-1}) $\langle m_B^{max} \rangle = 11.9$ mag (7)
All SNe	0.600	0.021	34	66	46	955
SNe in inclined galaxies	0.622	0.020	30	70	48	1005
SNe with $(B-V) > 0.2$ mag	0.631	0.021	25	71	49	1025
Only good SNe	0.659	0.030	10	76	52	1095
Upper limit	0.740	0.008	4	91	63	1320

NOTE.—Also given are the errors and number of SNe in the sample. The Hubble constant for the most extreme absolute magnitudes inferred from b are indicated.

those two parameters, and we can only give solutions for the two (extreme) cases where (1) the scatter in Figure 4 is dominated by the intrinsic dispersion of SNe Ia at maximum and extinction is negligible, and (2) the intrinsic luminosity function of SNe Ia at maximum is very narrow and the scatter is due mostly to absorption of the SNe. Case (1) (*middle line* in Fig. 4) is represented by the "good" sample in Table 3, but for case (2) (*upper line*) we calculated an upper limit for b by using the four SN 1959C, SN 1970J, SN 1974J, and SN 1980N which all lie at the upper boundary of the distribution (denoted as "upper limit" in Table 3).

The Hubble constant is calculated from b simply with (e.g., TL)

$$\log (H_0) = 0.2M_B + b + 5 . \quad (2)$$

We find that the largest contributor to the uncertainty in the value of H_0 derived from the observed Hubble diagram is the uncertainty in the intrinsic luminosity distribution (col. [5] and [6] in Table 3) which is as large as the combined uncertainties from the absolute magnitudes.

In Figure 3 we show the extreme scales for the Hubble constant as they depend on the models and the choice of Δt. The inner scale was calculated with b determined from the mean of the sample of "good" supernovae while the outer scale is calculated from the upper limit to b. It is striking to see what a difference the sample definition makes on H_0. The unknown selection effects thus clearly represent one of the biggest uncertainties in the derivation of H_0. We find rigorous limits for H_0, since other sources of uncertainty such as peculiar velocities, errors in the derivation of the observed peak magnitudes, and observational errors all contribute to the scatter in Figure 4 and are expected to have roughly symmetric distributions.

The upper limit to H_0 is about 90 km s^{-1} Mpc^{-1} by taking the faintest model with the longest rise time ($\Delta t = 22$ days) and assuming that absorption is the dominant source of scatter in the Hubble diagram. If, however, the scatter in Figure 4 is predominantly due to a dispersion in the intrinsic luminosities of SNe Ia at peak, we find $50 < H_0 < 75$. This exemplifies the rather extreme spread in values which results from differing assumptions about the biases involved. Even if we would be able to single out one explosion model, a considerable range for the Hubble constant remains.

While for the moment only weak limits can be derived for the Hubble constant with SNe Ia, there is room for significant improvement. Additional constraints on the theoretical models of SNe Ia, especially by synthetic spectra and light curves, and the firm determination of the appropriate Hubble line for SNe Ia in the Hubble diagram will eventually narrow the possible values for H_0 significantly.

5.2. *The Distance to Virgo and the Infall Velocity*

With the assumption that the depth of the Virgo Cluster is negligible compared with its distance, (see, however, Tonry, Ajhar, & Luppino 1990), values for the peak B brightness of SNe Ia in Virgo $m_B^{\rm Virgo}$ have been found to be 11.9 mag (LT) and 12.1 mag (Capaccioli et al. 1990). This second group, however, also finds a range of 12.2 mag $\geq m_B^{\rm Virgo} \geq$ 11.6 mag, depending on the assumed absorption law in the parent galaxies. The range in absolute magnitudes $M_B^{\rm max}$ derived above translates to extreme limits of the distance modulus for the Virgo Cluster $(m - M)_0$ of 30.8 ($M_B^{\rm max} = -18.9$) and 31.8 ($M_B^{\rm max} = -19.7$), respectively, and a distance between 14.5 and 22.9 Mpc. The lower limit on the Virgo distance is consistent with determinations which use planetary nebula luminosity functions (Jacoby, Ciardullo, & Ford 1990), surface brightness fluctuations (Tonry et al. 1990), and the Tully-Fisher method (Pierce & Tully 1988). Values from the long distance scale (e.g., Tammann 1988; Sandage & Tammann 1990), however, are well within the upper limit of our Virgo distance, and it conforms with other distance determinations of the Virgo Cluster (e.g., Branch 1988; Harris 1988; Bartel 1991; Schmidt, Kirshner, & Eastman 1992).

In principle, a sample of distant SNe and the mean apparent B magnitude of SNe Ia in Virgo provide the basis to measure the cosmic velocity $v_{\rm Virgo}$ (eq. [1]) of, and hence our infall toward, the Virgo Cluster (Sandage & Tammann 1990). We have calculated the range of possible $v_{\rm Virgo}$ from b in Table 3 (col. [7]). Note that this derivation is completely independent of any model assumption, but relies only on the value of b determined from distant SNe Ia and the mean apparent magnitude of SNe Ia in Virgo (cf. eq. [1]).

To find the infall velocities we must know the observed velocity of the Virgo Cluster. This, however, is still a topic of debate (for a discussion of this quantity see Huchra 1988 and Tammann 1988). While the mean heliocentric velocity is fairly well agreed upon (Huchra 1985; Binggeli, Tammann, & Sandage 1987; Huchra 1988), there remain significant discrepancies in the correction to the center of the Local Group (Yahil, Tammann, & Sandage 1977; Huchra 1988) increasing the differences of $v_{\rm Virgo}^{\rm obs}$ to $\sim$10%. The range covered by the different values of b is telling in that for the complete sample of supernovae we find a cosmic velocity for Virgo that is *smaller* than any determination of $v_{\rm Virgo}^{\rm obs}$. Even the set of "good" supernovae indicates a very small infall velocity ($\Delta v \approx 120$ km s^{-1}, if we assume an observed mean Virgo velocity of 972 km s^{-1} [Binggeli et al. 1987]). It is comparable, however, to what was found by Sandage & Tammann (1990) and Faber & Burstein (1988). A rigorous upper limit is set by the upper limit in b at $v_{\rm Virgo} = 1320$ km s^{-1}. Thus, we find a range of allowed infall velocities of $0 < \Delta v < 350$ km s^{-1}, but are not able to narrow this range any further.

The sensitivity of the derived infall velocity to changes in the available data is also illustrated by the result of using $m_B^{\rm Virgo} =$ 12.1 as the mean observed peak magnitude of SNe Ia (Capaccioli et al. 1990). This changes all the values in Table 3 by $\sim$10% and increases the range to $1030 \lesssim v_{\rm Virgo} \lesssim 1450$ km s^{-1}, and consequently the infall velocities to $60 < \Delta v < 470$ km s^{-1}. We are clearly in need of more SNe Ia in the Virgo Cluster, if we are to improve the assessment of Δv.

6. CONCLUSIONS

Using as few assumptions as possible, we have derived limits for the luminosity of SNe Ia near maximum without resorting to the cosmic distance ladder. The fundamental assumptions in our calibration of the SN Ia distance scale are the following.

1. The progenitors of SNe Ia are Chandrasekhar-mass white dwarfs that are disrupted by explosive burning to NSE.
2. The light curve at late times is powered by the instaneous thermalization of the decay energy of radioactive ^{56}Co.
3. The luminosity distribution of SNe Ia at peak is narrow enough that they define the Hubble line in the Hubble diagram. Selection biases are suppressed by the small scatter in absolute magnitudes.

All other assumptions are connected with the treatment of details; we have chosen to present extreme cases for each to illustrate the effects these assumptions have on our calibration.

There are, however, several systematic uncertainties that for the moment prevent a more precise determination of the Hubble constant through this route.

The bolometric light curve is constructed from observations including only the optical and near-infrared emission. Our comparison with the luminosity determined by γ-ray deposition calculations thus assumes that the far-UV and mid- and far-infrared emission contribute insignificantly to the total. Since to date spectrum and light curve models are not sufficiently persuasive to narrow the range of models used in the determination of the luminosity, we chose a conservative approach and included the most extreme cases in these calculations. The rise time of SNe Ia remains undetermined, but does not strongly influence the results. A last theoretical uncertainty is the time at which the γ-ray deposition model first becomes appropriate. The identical slopes of the bolometric and the theoretical light curves after ~ 60 days past explosion indicate that the comparison at these epochs is well justified.

The procedure outlined above, however, circumvents several problems formerly encountered in the calibration of SNe Ia at maximum (ABW; Branch 1992). The use of a bolometric light curve assembled from observations of several supernovae frees us from any assumptions on the detailed spectral emission at maximum and avoids complicated radiation hydrodynamic calculations. The comparison with observed peak magnitudes is greatly facilitated in this manner. No assumption about the temperature at maximum or line blanketing is necessary. Further, the comparison of the light curves at phases where γ-rays are the only source for the supernova's luminosity relies on a relatively simple theoretical model. No knowledge is required of the optical opacity in the envelope which determines the detailed shape and luminosities of the peak in the models.

One main uncertainty remaining for the Hubble constant is the nature of the scatter in the Hubble diagram of SNe Ia at maximum (Fig. 4). Absorption is clearly an important contributor to this scatter as are the peculiar velocities at small distances. Extinction toward SNe Ia has been discussed in several contexts (Jöeveer 1982; Capaccioli et al. 1990; Della Valle & Panagia 1992; LT92; see, however, van den Bergh & Pierce 1992), and remains a major puzzle. Most of these authors favor an unconventional absorption law for SNe Ia, but no general agreement on its exact form has been reached. The close connection with the intrinsic luminosity distribution causes the biggest uncertainty in the determination of H_0. An independent determination of either quantity would be of great importance. An additional complication for the use of SNe Ia as standard candles is the recognition of peculiar SNe Ia like SN 1991bg in the elliptical galaxy NGC 4374 (Filippenko et al. 1992; Leibundgut et al. 1993). Such intrinsically dim SNe Ia have to be excluded, but the distinct signatures of these events should allow us to separate them from the bulk of "normal" SNe Ia. The selection by light curve shape, as employed here, is certainly a valid criterion.

The determination of the Hubble constant with SNe Ia remains unsatisfactory. Our limits on H_0 after inclusion of the uncertainty of the bolometric light curve are 45 km s^{-1} Mpc^{-1} at the lower end and 105 km s^{-1} Mpc^{-1} for the short distance scale. Although rigorous, they do not distinguish between the two commonly discussed values. The link between the white dwarf models of SNe Ia and the Hubble constant, however, opens up an interesting new connection; should the Hubble constant turn out to be outside the limits supported by the models, the generic picture of SN Ia explosions would have to be revised.

The range of H_0 can be reduced considerably by tackling the various uncertainties. Infrared and ultraviolet observations as well as R and I light curves will fill in the missing emission in the bolometric light curve. Integration of spectrophotometry as accomplished for SN 1987A (Bouchet et al. 1991) will define the bolometric light curve even better as the data sets become available (e.g., Wells et al. 1993 [SN 1989B]; Phillips et al. 1992; Filippenko et al. 1992 [SN 1991T]). Deep searches for SNe will provide an extension of the Hubble diagram to larger distances where the role of peculiar velocities is greatly diminished and will provide observations at earlier phases as the chance of finding a nearby supernova very early is increased. This will help to better define the Hubble diagram and decrease the uncertainty in Δt. Finally, we should strive to improve our knowledge of extinction in external galaxies and its effect on SNe. This will then allow us to define the luminosity function of SNe Ia at maximum.

We would like to thank M. Franx, R. Kirshner, and S. Woosley for useful discussions of several of the presented topics. S. Woosley kindly provided his explosion models prior to publication. We are indebted to the referee, D. Branch, for pointing out an error to us and for comments which substantially helped to improve the presentation of this paper. This research has been supported through grants AST 89-05529 (B. L.) and NASA GRO/PFP-91-29 (P. A. P.).

REFERENCES

Arnett, W. D. 1982, ApJ, 253, 785
Arnett, W. D., Branch, D., & Wheeler, J. C. 1985, Nature, 314, 337 (ABW)
Axelrod, T. S. 1980, Ph.D. thesis, University of California at Santa Cruz
Barbon, R., Ciatti, F., & Rosino, L. 1973, A&A, 25, 65
Bartel, N. 1991, Supernovae, ed. S. E. Woosley (New York: Springer), 760
Binggeli, B., Tammann, G. A., & Sandage, A. 1987, AJ, 94, 251
Blair, W. P., & Panagia, N. 1987, in Exploring the Universe with the *IUE* Satellite, ed. Y. Kondo et al. (Dordrecht: Kluwer), 549
Bouchet, P., Phillips, M. M., Suntzeff, N. B., Gouiffes, C., Hanuschik, R. W., & Wooden, D. H. 1991, A&A, 245, 490
Bragaglia, A., Greggio, L., & Renzini, A. 1991, SN 1987A and Other Supernovae, ed. I. J. Danziger & K. Kjär (Garching: ESO), 47
Bragaglia, A., Greggio, L., Renzini, A., & D'Odorico, S. 1990, ApJ, 365, L13
Branch, D. 1982, ApJ, 258, 35
———. 1988, The Extragalactic Distance Scale, ed. S. van den Bergh & C. J. Pritchett (San Francisco: ASP), 146
———. 1992, ApJ, 392, 35
Branch, D., & Bettis, C. 1978, AJ, 83, 224
Branch, D., Drucker, W., & Jeffery, D. J. 1988, ApJ, 330, L117
Buta, R. J., & Turner, A. 1983, PASP, 95, 72
Cadonau, R., Sandage, A., & Tammann, G. A. 1985, Supernovae as Distance Indicators, ed. N. Bartel (Berlin: Springer), 151
Capaccioli, M., Cappellaro, E., Della Valle, M., D'Onofrio, M., Rosino, L., & Turatto, M. 1990, ApJ, 350, 110
Clayton, D. D. 1974, ApJ, 188, 155
Colgate, S. A., & McKee, C. 1969, ApJ, 157, 623
Della Valle, M., & Panagia, N. 1993, AJ, 104, 696
Eastman, R. E., & Pinto, P. A. 1993, ApJ, in press
Elias, J. H., Matthews, K., Neugebauer, G., & Persson, S. E. 1985, ApJ, 196, 379
Faber, S. M., & Burstein, D. 1988, in Large-Scale Motions in the Universe, ed. V. C. Rubin & G. V. Coyne (Princeton: Princeton Univ. Press), 115
Filippenko, A. V., et al. 1992, AJ, in press
Frogel, J. A., Gregory, B., Kawara, K., Laney, D., Phillips, M. M., Terndrup, D., Vrba, F., & Whitford, A. E. 1987, ApJ, 315, L129
Fukugita, M., & Hogan, C. J. 1991, ApJ, 368, L11

Graham, J. R. 1987, ApJ, 315, L129
Hamuy, M., Phillips, M. M., Maza, J., Wischnjewsky, M., Uomoto, A., Landolt, A. U., & Kathwani, R. 1991, AJ, 102, 208
Harkness, R. P. 1991a, in Supernova, ed. S. E. Woosley (New York: Springer), 454
———. 1991b, in SN 1987A and Other Supernovae, ed. I. J. Danziger & K. Kjär (Garching: ESO), 447
Harkness, R. P., & Wheeler, J. C. 1990, in Supernovae, ed. A. G. Petschek (New York: Springer), 1
Harris, W. E. 1988, in The Extragalactic Distance Scale, ed. S. van den Bergh & C. J. Pritchett (San Francisco: ASP), 231
Huchra, J. P. 1985, in The Virgo Cluster, ed. O.-G. Richter & B. Binggeli (Garching: ESO), 181
———. 1988, in The Extragalactic Distance Scale, ed. S. van den Bergh & C. J. Pritchett (San Francisco: ASP), 257
Iben, I., Jr., & Tutukov, A. V. 1984, ApJS, 54, 335
Jacoby, G. H., Ciardullo, R., & Ford, H. C. 1990, ApJ, 356, 332
Jeffery, D. J., Leibundgut, B., Kirshner, R. P., Benetti, S., Branch, D., & Sonneborn, G. 1992, ApJ, 397, 304
Jöeveer, M. 1982, Astrofizika, 18, 574
Khokhlov, A., Müller, E., & Höflich, P. 1992, A&A, 253, L9
Kirshner, R. P., & Oke, J. B. 1975, ApJ, 200, 574
Kowal, C. T. 1968, AJ, 73, 1021
Kraan-Korteweg, R. C. 1986, A&AS, 66, 255
Lee, T. A., Wamsteker, W., Wisniewski, W. Z., & Wdowiak, T. J. 1972, ApJ, 177, L59
Leibundgut, B. 1988, Ph.D. thesis, University of Basel
———. 1990, A&A, 229, 1
———. 1991, Supernovae, ed. S. E. Woosley (New York: Springer), 751
Leibundgut, B., Kirshner, R. P., Filippenko, A. V., Shields, J. C., Foltz, C. B., Phillips, M. M., Sonneborn, F. 1991b, ApJ, 371, L23
Leibundgut, B., & Tammann, G. A. 1992, in preparation (LT92)
———. 1990, A&A, 230, 81 (LT)
Leibundgut, B., Tammann, G. A., Cadonau, R., & Cerrito, D. 1991a, A&AS, 89, 537
Leibundgut, B., et al. 1993, AJ, in press
Miller, D. L., & Branch, D. 1990, AJ, 100, 530
———. 1992, AJ, 103, 379
Nomoto, K., Thielemann, F.-L., & Yokoi, K. 1984, ApJ, 286, 644
Panagia, N. 1982, Proc. 3rd European IUE Conference (ESA-SP176), 31
Phillips, M. M., Wells, L. A., Suntzeff, N. B., Hamuy, M., Leibundgut, B., Kirshner, R. P., & Foltz, C. B. 1992, AJ, 103, 1632
Phillips, M. M., et al. 1987, PASP, 99, 592
Pierce, M. J., & Tully, R. B. 1988, ApJ, 330, 579
Pinto, P. A. 1988, Ph.D. thesis, University of California at Santa Cruz
Pinto, P. A., & Woosley, S. E. 1988, ApJ, 329, 820
Pskovskii, Y. P. 1968, Sov. Astron., 11, 570
———. 1971, Sov. Astron., 14, 798
Sandage, A., & Tammann, G. A. 1990, ApJ, 365, 1
Schmidt, B. P., Kirshner, R. P., & Eastman, R. G. 1992, ApJ, 395, 366
Shigeyama, T., Nomoto, K., Yamaoka, H., & Thielemann, F.-K. 1992, ApJ, 386, L13
Suntzeff, N. B., Phillips, M. M., Depoy, D. L., Elias, J. H., & Walker, A. R. 1991, AJ, 102, 1118
———. 1992, ApJ, 384, L33
Tammann, G. A. 1978, in Astronomical Uses of the Space Telescope, ed. F. Macchetto, F. Pacini, & M. Tarenghi (Garching: ESO), 329
———. 1982, in Supernovae: A Survey of Current Research, ed. M. J. Rees & R. J. Stoneham (Dordrecht: Reidel), 371
———. 1988, in The Extragalactic Distance Scale, ed. S. van den Bergh & C. J. Pritchett (San Francisco: ASP), 282
Tammann, G. A., & Leibundgut, B. 1990, A&A, 236, 9 (TL)
Tonry, J. L., Ajhar, E. A., & Luppino, G. A. 1990, AJ, 100, 1416
Trimble, V. 1982, Rev. Mod. Phys., 54, 1183
———. 1991, A&AR, 3, 1
Tully, B. R. 1988, Nearby Galaxies Catalogue (Cambridge: Cambridge Univ. Press)
van den Bergh, S. 1988, in The Extragalactic Distance Scale, ed. S. van den Bergh & C. J. Pritchett (San Francisco: ASP), 221
van den Bergh, S., & Pazder, J. 1992, ApJ, 390, 34
van den Bergh, S., & Pierce, M. J. 1992, PASP, 104, 408
van den Bergh, S., & Pritchett, C. J., ed. 1988, The Extragalactic Distance Scale (San Francisco: ASP)
Wells, L. A., et al. 1993, in preparation
Weaver, T. A., Axelrod, T. S., & Woosley, S. E. 1980, Type I Supernovae, ed. J. C. Wheeler (Austin: Univ. of Texas), 113 (WAW)
Wheeler, J. C., & Harkness, R. P. 1990, Rep. Prog. Phys., 53, 1467
Woosley, S. E. 1988, ApJ, 330, 218
———. 1991, Gamma-Ray Line Astrophysics, ed. P. Durouchoux & N. Prantzos (New York: American Institute of Physics), 270
Woosley, S. E., Pinto, P. A., & Ensman, L. M. 1988, ApJ, 324, 466
Woosley, S. E., Pinto, P. A., & Hartmann, D. 1989, ApJ, 346, 395
Woosley, S. E., Taam, R. E., & Weaver, T. A. 1986, ApJ, 301, 601
Woosley, S. E., & Weaver, T. A. 1986, ARA&A, 24, 205
Yahil, A., Tammann, G. A., & Sandage, A. 1977, ApJ, 217, 903